GROWTH DYNAMICS OF MITOCHONDRIA IN SYNCHRONIZED CHINESE HAMSTER CELLS

DENNIS W. ROSS *and* HOWARD C. MEL

From the Division of Medical Physics and Group in Biophysics, Donner Laboratory, University of California, Berkeley, California 94720

ABSTRACT The increase in cell volume (from electronic cell sizing) and the apportionment of this volume amongst the nuclear, cytoplasmic, and mitochondrial subcellular compartments (from electron microscopy) were studied throughout the cell division cycle in partially synchronized cultures of Chinese hamster V79-S171 cells. Average whole cell volume was found to increase smoothly, consistent with the doubling in one generation of individual cell volume. Nuclear size increased in like fashion. Mean total mitochondrial volume and number of mitochondria per cell both showed a different kind of variation, most notably a significant decrease in G_1 and G_2 as compared with mid S. These results are therefore counter to a model of simple doubling of mitochondria either synchronously with the cell division cycle or asynchronously. Absolute mean values per cell for log phase Chinese hamster cells were also determined, as follows: whole cell volume, 710 μ^3; nuclear volume, 190 μ^3; total mitochondrial volume, 37.5 μ^3; number of mitochondria per cell, 90.

INTRODUCTION

The mammalian cell division cycle encompasses a complicated series of events involving the maintenance of cell metabolism and the orderly increases in all subcellular components necessary for a parent cell to divide into two daughter cells. Techniques of synchronizing cultures of cells and then observing these growth events as a function of time have provided a powerful approach to elucidating the steps in synthesis and subcellular organization necessary for cell division.

In an earlier investigation with synchronized Chinese hamster cells, smooth doubling (with time) of the average cell volume, as a daughter cell grows to become the next parent cell, was reported (Sinclair and Ross, 1969). The present study is concerned with questions surrounding the biogenesis of mitochondria for these same cells. Specifically, is mitochondrial replication closely linked to steps in the cell cycle or are mitochondria autonomously replicating organelles? How do mitochondrial numbers and volume change during the cell division cycle, and do such changes correlate with changes in mitochondrial activity, such as those reported by Cottrell and Avers (1971) and Bosman (1971)?

This communication presents experimental findings of a study of the growth dynamics of mitochondria during the cell cycle of Chinese hamster cells. Based primarily on electron microscopic techniques, it clarifies how the increase in total cell volume is apportioned between the subcellular compartments of nucleus, mitochondria, and surrounding cytoplasm and hence provides at least partial answers to some of these questions.

MATERIALS AND METHODS

Cell Culture

The cells used were the V79-S171 line of Chinese hamster cells with a generation time of 9.5 hr, subdivided into a pre-DNA synthetic period G_1 of 1.5 hr, a DNA synthetic period S of 6 hr, a post-DNA synthetic period G_2 of 1.5 hr, and mitosis lasting 0.5–1 hr. Cells were grown in monolayer cultures attached to the surface of plastic dishes at 37°C in Minimal Essential Medium, Earle's (Microbiological Associates, Inc., Bethesda, Md.) supplemented with 15% v/v fetal calf serum (Grand Island Biological Co., Grand Island, N.Y.) in a humid atmosphere of 2% CO_2 and air. Synchronous cells were obtained from asynchronous log phase cultures by selection for loosely attached dividing cells using a modification of the shake-off procedure described by Sinclair and Morton (1963). In our experiments, pre-chilling the cells before shake-off was not employed and cell medium rather than trypsin was used for the shake-off itself. This procedure of agitating log phase cell cultures selectively causes the loosely attached rounded cells which are about to divide to be shaken loose into suspension. Portions of the resulting suspension of synchronous cells were inoculated into a series of dishes and incubated at 37°C.

Cell Volume and DNA Synthesis

The percentage of cells synthesizing DNA and average cell volume were monitored during the cell cycle as a check on the quality of synchrony and on the timing of the cell cycle. At five intervals throughout the next 10 hr, portions were removed and labeled with a 15 min pulse of tritiated thymidine (0.1 μCi/ml; 14 Ci/mmole) followed by a radioautographic procedure to determine the number of cells engaged in DNA synthetic activity (Ford and Yerganian, 1958; Ross and Sinclair, 1972). Other portions were removed at the same times and the cells were detached from the Petri dish surface by treatment with trypsin (0.03% v/v, Grand Island Biological Co.). These cell suspensions were sized electronically and then fixed and prepared for electron microscopy. The sizing of cell suspensions was done using a cell volume spectrometer consisting of a 100 μ diameter aperture (Particle Data Inc., Elmhurst, Ill.) with amplification and accessory electronics of our laboratory design, and pulse height analysis performed by a PDP-8/I computer on-line (Digital Equipment Corp., Maynard, Mass.).

Electron Microscopy

Cells were initially fixed for approximately 24 hr in a 1% w/v solution of osmium tetroxide in 0.1 M sodium cacodylate buffer, adjusted to pH 7.4 at 4°C. The fixed cells were then dehydrated through sequential alcohols to absolute ethanol, moved to propylene oxide, and then embedded in Epon 812 using DMP 30 catalyst. Sections of 600–800 A thickness were cut on an MT-2 microtome (Ivan Sorvall, Inc., Norwalk, Conn.). The sections were picked

up on 200-mesh copper grids and stained with a saturated aqueous solution of uranyl acetate (6% w/v) for 30 min, then with Reynold's lead citrate solution for 15 min. Electron micrographs were made of the sections at a final magnification of ×11,500 (model HU-11 electron microscope, Hitachi Instruments, Kyoto, Japan).

Analysis of Electron Micrographs

The quantitative determination of cellular and subcellular dynamics from electron micrographs of populations of cells requires careful attention to technique plus the validity of certain assumptions. On each electron micrograph the whole cell cross-sectional area was partitioned into nuclear, mitochondrial, and cytoplasmic components on the basis of the distinguishable morphology of each of these components. This was done for all sections of cells appearing on the photograph, including portions of cells cut off by the edge of the photograph and sections which did not include any portion of the nucleus. The cross-sectional area of each component was then determined using a polar planimeter by tracing separately the perimeter of the whole cell and the perimeter of the nucleus. The area of each mitochondrion was determined by measuring the major and minor axes and computing the area of the equivalent ellipse. The number of mitochondria within each measured area of cytoplasm was also noted. Mitochondrial sections larger than 2 mm in diameter (on the photograph) were recorded; smaller sections than these could not be reliably recognized as mitochondria.

At each experimental point approximately fifteen 8 × 10 inch photographs representing 6000 μ^2 of cell area were studied. Each photograph was taken of a random field chosen blindly so as to avoid arbitrarily selecting "eye-catching" fields. (For example, the eye would be automatically drawn to fields with a large nucleus, since on the electron microscope viewing screen this forms a marked area of contrast. Preferential selection of such fields would clearly lead to a bias in the ratio of observed nuclear to cytoplasmic area.) Care was also taken to select sections from the embedding pellet so that no two sections were cut within 20 μ (about two cell diameters) of each other, thus insuring that each section was cut through a different group of cells.

RESULTS

The results of the progression with time of (*a*) the percentage of cells labeled with tritiated thymidine as determined by radioautography (per cent labeled index) and (*b*) the average cell volume are shown in Figs. 1 *a* and 1 *b*, respectively. The solid lines through the data points are the predictions of a computer model of the synchronized population based on the distribution of cell generation times (see Sinclair and Ross, 1969). These quantities were monitored as a check on the quality of synchrony and on the timing of the cell cycle. A high yield of cells from the synchrony procedure was necessary to produce the 5×10^6 cells required for this experiment which led to a corresponding sacrifice in the best quality of synchrony normally attained by the mitotic selection procedure. The synchrony as measured by the labeling index (Fig. 1 *a*) showed a rise from only 30 to 68% with the data fit by a mathematical model assuming a 30% coefficient of variation in the distribution of cell generation times. The same experiment showed considerably better synchrony in terms of cell volume changes (Fig. 1 *b*), with the data fit assuming a 15% coeffi-

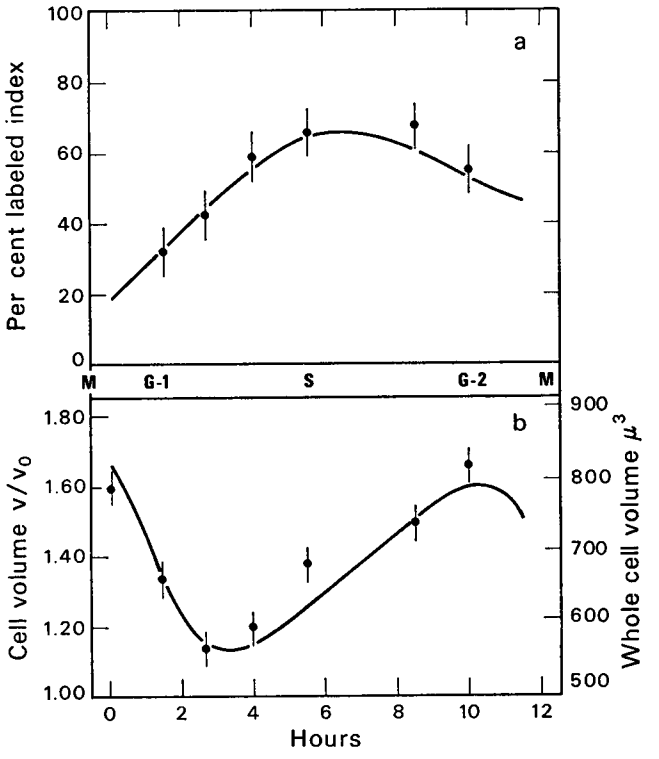

FIGURE 1 (*a*) Per cent labeled cells by tritiated thymidine incorporation, and (*b*) mean cell volume (relative units and cubic microns) vs. time for synchronized Chinese hamster V79-S171 cells. Points are experimental results with error bars denoting the Poisson statistical uncertainty of 1 SD (equation 1). Solid curves drawn through the data points are the predictions of a computer model for the synchronized population (Sinclair and Ross, 1969).

cient of variation in the distribution of cell generation times. Also the G_1 period of the cell cycle was found to be 3 hr long rather than the normal 1.5 hr characteristic of this cell line. Such a delay in G_1 has been noted on several occasions after a large shake-off procedure as a consequence of longer times required in handling large cell batches. After this induced delay, the events in the cell cycle proceeded with normal timing.

The results of measurements of the individual subcellular component areas are expressed as the *nuclear area fraction* $N/(N + M + C)$ and the *mitochondrial area fraction* $M/(N + M + C)$ where N, M, and C are the nuclear, mitochondrial, and cytoplasmic areas respectively. The *mitochondrial number density* was also measured and is denoted as $M_N/(N + M + C)$, where M_N is the number of mitochondria observed within the whole cell area $(N + M + C)$. The uncertainty in the mean value obtained for each of these ratios is derived from the Poisson statistical uncertainty of counting individual units of area. Specifically the range of the standard

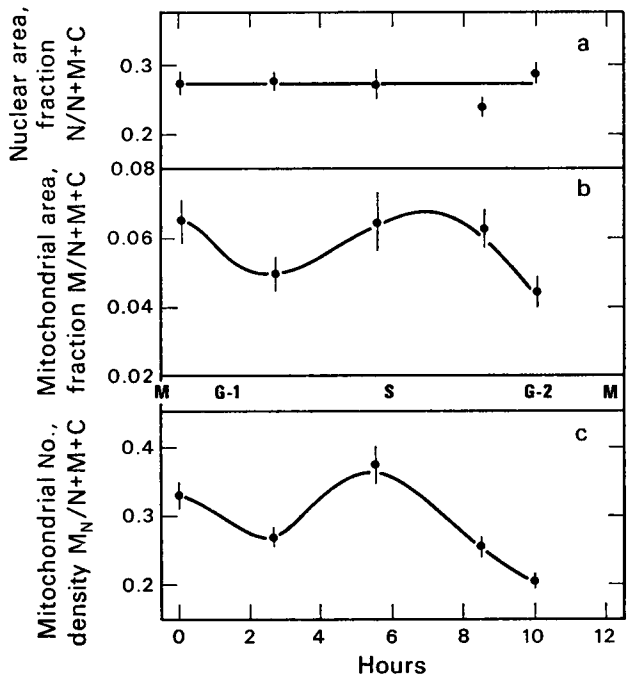

FIGURE 2 (*a*) Nuclear area fraction $N/(N + M + C)$; (*b*) Mitochondrial area fraction $M/(N + M + C)$; and (*c*) Mitochondrial number density $M_N/(N + M + C)$ vs. time for synchronized Chinese hamster V79-S171 cells, same experiment as Fig. 1. Error bars about the experimental points denote the Poisson statistical uncertainty of 1 SD derived from counting individual units of area. Solid curves were fitted by eye.

deviation in the ratio X/Y is given by:

$$\Delta(X/Y) = \pm (X \pm \sqrt{X})/(Y \mp \sqrt{Y}). \quad (1)$$

15 photographs sampling 6000 μ^2 of cell area was sufficient to achieve a standard deviation of less than 10% of the value of the mean.

The measurements of the individual subcellular component areas were derived from examining approximately 6000 mitochondria in 500 cells (or portions of cells) in 100 photographs. The results are shown in Figs. 2 *a*, 2 *b*, and 2 *c* as a function of time during the cell cycle. The approximate timing of the phases of the cell cycle as determined from the results of Fig. 1 is also shown.

The partitioning of the increase in cell volume during the cell cycle into subcellular compartments of nucleus, mitochondria, and cytoplasm occurs in such a way that the nuclear area fraction $N/(N + M + C)$ remains constant, i.e., the nucleus changes in size at the same pace as the whole cell. The mitochondrial area fraction $M/(N + M + C)$, however, shows a significant decrease in G_2 compared with its value in mid S (Fig. 2 *b*), and a parallel change is also seen in the independent

parameter, the mitochondrial number density $M_N/(N + M + C)$ (Fig. 2 *c*). Chi-squared test of goodness of fit shows that the last data point at $t = 10$ hr (G_2) in Fig. 2 *b* deviates significantly from a (horizontal) straight line obtained from a least squares fit through the first four points ($P < 0.1$). Similarly the curve of Fig. 2 *c* significantly deviates from a straight line least squares fit through all five data points ($P < 0.001$). The curve for the nuclear area fraction vs. time (Fig. 2 *a*), however, is fit by such a straight line ($P > 0.95$).

A more intuitive and quantitatively useful form of the data can be obtained by converting the nuclear and mitochondria area fractions into absolute volumes. This is accomplished by a mathematical method described in the Appendix. The results of those calculations are given in the form of mean nuclear volume $\mathfrak{N}$ mean total mitochondrial volume per cell $\mathfrak{M}$, and average number of mitochondria per cell $\mathfrak{M}_N$ vs. time in the synchronized cell division cycle, Figs. 3 *a*, 3 *b*, and 3 *c*, respectively.

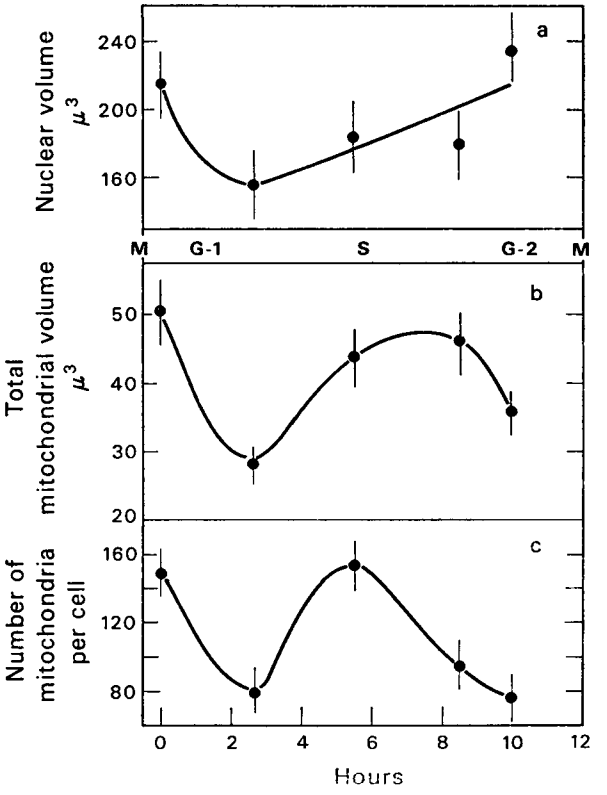

FIGURE 3 (*a*) Mean nuclear volume μ^3; (*b*) mean total mitochondrial volume μ^3; and (*c*) average number of mitochondria per cell vs. time for synchronized Chinese hamster V79-S171 cells. Error bars about the experimental points denote Poisson statistical uncertainty of 1 SD derived from counting individual units of area. Solid curves were fitted by eye.

TABLE I

WHOLE CELL AND ORGANELLE VOLUMES FOR ASYNCHRONOUS CHINESE HAMSTER CELLS

Mean whole cell volume	710	$\pm 25\ \mu^3$
Mean nuclear volume	190	$\pm 20\ \mu^3$
Total mitochondrial volume	37.5	$\pm\ 5\ \mu^3$
Mean number of mitochondria/cell	90	$\pm\ 2\ \mu^3$
Mean volume per mitochondrion	0.423	$\pm\ 0.15\ \mu^3$

The mean values of the nuclear volume, total mitochondrial volume, and number of mitochondria per cell for an *asynchronous* log phase population of Chinese hamster V79-S171 cells were determined by pooling (appropriately weighted) data for all experiments (see Ross, 1972). The values for nuclear and mitochondrial volumes and numbers obtained are given in Table I. The uncertainty of each of the values given in Table I is estimated by a propagation of errors formula that includes the 3% imprecision in the calibration of the electronic sizing procedure and the 10% error in determining the organelle area fractions. These latter two errors are the standard deviation due to Poisson counting statistics (see equation 1). The limits in Table I thus represent the uncertainties in determining the mean values of these parameters rather than the range of variation in the cell population.

DISCUSSION

The evidence obtained in this study suggests that while the nucleus increases in size in pace with whole cell growth, the mitochondria exhibit a more complex kinetics. The observed changes in mitochondria represent an appearance and disappearance of structures recognizable as morphologically intact mitochondria. In eucaryotic cells mitochondria have been thought to have originated as parasites as evidenced by their many similarities to bacteria (Cohen, 1970), though in yeast, they have been shown to be dependent on nuclear genes (Roodyn and Wilkie, 1968). These ideas suggest a simple model of mitochondrial replication by binary division, either synchronously or asynchronously, leading to a doubling within one generation time. Our findings of a significantly decreased mitochondrial volume and number in G_2 when the cell is approaching its maximum volume before division are not consistent with such a model.

In yeast it is known that mitochondria can undergo a reversible reduction to promitochondria when exposed to anaerobic conditions (Linnane et al., 1968). Such promitochondria are normally not recognizable under the electron microscope. The decreases in mitochondria which we observed could be due to a similar mechanism whereby mitochondria not in an active state are not morphologically recognizable. Other hypotheses of mitochondrial dynamics, such as disassembly and assembly by the cell itself (rather than autonomous division) are also consistent with the data.

Studies on mitochondrial dynamics in synchronized microbial cultures demonstrate that no single hypothesis of mitochondrial biogenesis is consistent with all the observed patterns. Osumi and Sando (1969) report, from a light and electron microscopic study of synchronized cultures of *Schizosaccharomyces pombe*, that nuclear division begins at one-fifth and ends at four-fifths of the cell cycle, while mitochondrial division begins at two-fifths and ends at three-fifths of the cycle. Cottrell and Avers (1971) find a different pattern in synchronized *Saccharomyces cerevisiae* which they cannot account for in terms of such a model of synchronized mitochondrial division. They find a linear increase during the cell cycle in numbers of mitochondria per electron microscopic field, which they interpret as a constant nonsynchronous biogenesis of mitochondria. In *Neurospora*, Hawley and Wagner (1967) report increases in numbers of mitochondria synchronous with mitotic activity.

Studies in mammalian cells on the variation in actual numbers or volumes of mitochondria are sparse despite the early work by Allard et al. (1952 *a*, *b*). Using a light microscopic technique these authors observed an increase with time in numbers of mitochondria in regenerating rat liver cells. More recently in a quantitative study of electron micrographs of normal human liver biopsy material Tauchi and Sato (1966) describe a decrease in number but an increase in size of mitochondria with advancing age.

Biochemical events associated with mitochondrial biogenesis during the cell division cycle have been more completely investigated. Thus for Chang liver cells synchronized by cold shock the rate of synthesis of mitochondrial DNA has been observed to be maximal in G_2 (Koch and Stockstad, 1967). For mouse L5178Y cells synchronized by excess thymidine and Colcemid, Bosman (1971) found the rate of mitochondrial DNA synthesis to be greatest in S and G_2. This was also just found to be the case for HeLa cells synchronized by mitotic selection (Pica-Mattoccia and Attardi, 1972). When a double thymidine block, however, was used by these same experimenters no cyclic variation in mitochondrial DNA synthesis was seen. Rabinowitz and Swift (1970) have reviewed many of the experiments on mitochondrial nucleic acids and discussed their relation to the problem of mitochondrial biogenesis. An important variable in these studies, however, is the unknown effects on the mitochondrial population of the physical and chemical methods of synchrony used. We felt it desirable to use a *selection* procedure for synchronization in order to minimize introduction of an unknown perturbation in the mitochondrial dynamics. Despite a sacrifice in quality of synchrony obtained due to the requirements of a high yield of cells, a significant change in mitochondrial dynamics was observed. Technical improvements in the research methods including less tedious procedures for measuring mitochondrial volume and number coupled with improved synchrony, however, are a desirable future goal. Isolation of mitochondrial fractions from synchronized cells, with subsequent electronic counting

and sizing, and microspectrophotometric studies on vitally stained mitochondria are two possible experimental techniques that may be applicable to this problem.

Further studies are also clearly indicated to relate mitochondrial dynamics as observed here to mitochondrial metabolism during the cell cycle. There is also a pressing need to clarify the physical mode of replication of mitochondria in order to elucidate a more complete picture of the relationship between the whole cell and its organelles.

The authors gratefully acknowledge the assistance with electron micrographs provided by Mrs. Frances Taylor, and also the assistance in scanning photographs and data processing performed by Mr. Stephen Akeson.

Dr. Mel was supported by Atomic Energy Commission contract No. W-7405-eng-48.

Received for publication 11 April 1972 and in revised form 21 June 1972.

APPENDIX

Derivation of Absolute Organelle Volumes

The actual volumes of the nucleus and mitochondria can be estimated from the respective area fractions plus a knowledge of the average whole cell volumes as determined by the electronic sizing method. The area fractions represent the average nuclear and mitochondrial areas per element of whole cell cross-sectional area in randomnly oriented sectional planes through the cells. Calculations of the nuclear volume are performed by referencing the cell with respect to an axis perpendicular to the nuclear areas in the serial cross sections and integrating over this area. That is

$$\mathfrak{N} = \int [N/(N + M + C)]_z A(z)\, dz, \tag{2}$$

where $\mathfrak{N}$ is the volume of the nucleus; $A(z)$ is the cross-sectional area of the cell as a function of distance along the z axis; and $[N/(N + M + C)]_z$ is the nuclear area fraction in that cross-section. In order to use equation 2 for our data we replace the function, nuclear area fraction, by our measured mean value obtained for the nuclear area fraction from many randomly oriented planes. Thus equation 2 becomes:

$$\bar{\mathfrak{N}} = N/(N + M + C) \int A(z)\, dz, \tag{3}$$

where $\bar{\mathfrak{N}}$ is the mean nuclear volume.

The integral portion of equation 3 is simply the mean whole cell volume $\bar{v}$. Thus equation 3 is equivalent to:

$$\bar{\mathfrak{N}} = [N/(N + M + C)]\bar{v}. \tag{4}$$

Similarly for the mean total mitochondrial volume within a cell:

$$\bar{\mathfrak{M}} = [M/(N + M + C)]\bar{v}. \tag{5}$$

The absolute mean whole cell volume $\bar{v}$, in cubic microns, is calculated from the electronically measured relative volumes v/v_0 (see Fig. 1 *b*) by the expression:

$$\bar{v} = (710\ \mu^3/1.44 \text{ relative units})\ v/v_0\,. \tag{6}$$

The multiplicative factor in equation 6 is determined from calibration of the electronic volume sizing apparatus. This calibration factor is obtained by matching mean experimental volume (710 μ^3) with the theoretical mean cell volume of $v/v_0 = 1.44$ for a population with an exponential mode of volume increase. (The mean log phase cell volume of 710 μ^3 was determined by optical sizing of 700 cells as reported in an earlier study, see Sinclair and Ross, 1969).

It is also possible to estimate the total number of mitochondria per cell from the number density per cross sectional area. The *volume* number density is simply the *area* density raised to the 3/2 power hence:

$$\bar{\mathfrak{N}}_N = [M_N/(N + M + C)]^{3/2}\bar{v} \tag{7}$$

Note that this calculation does not require counting the number of cells or nuclei on the electron micrographs; it depends only on the number of mitochondria per unit area on the photographs and the electronically determined whole cell volume.

These formulas for absolute volumes and number do not include corrections for two second-order effects. Firstly, these derivations assume infinitely thin sections, whereas actual sections were between 600 and 800 A thick. Thus mitochondria within a given cross-sectional cut may not all be within the same mathematical plane, leading to an overestimation of total mitochondrial volume by equation 5 and also of the mitochondrial number by equation 7. The size of this second-order effect can be estimated as follows: the number density of mitochondria per cell area, averaged for all experimental data is $0.25/\mu.^2$ This implies an average nearest neighbor distance between mitochondria of $(1/0.25)^{1/2}$ or 2 μ. Since the sectional thickness is only one-third this average distance, the "overcounting" will be small. A second factor affecting the accuracy of equation 7 but in the opposite direction, is the fact that mitochondrial sections smaller than 2 mm in diameter on electron micrographs were not counted because they have too indistinct a morphology to be scored as mitochondria. (The range of mitochondrial section diameters seen in the electron micrographs was 2–20 mm, with a mean of 6 mm.) For an average mitochondrion represented by a 1-μ diameter sphere, the correction due to section thickness is less than 2%.

REFERENCES

ALLARD, C., R. MATHIEU, G. DE LAMIRANDE, and A. CANTERO. 1952 *a*. *Cancer Res.* **12**:407.

ALLARD, C., R. MATHIEU, G. DE LAMIRANDE, and A. CANTERO. 1952 *b*. *Cancer Res.* **12**:580.

BOSMAN, H. B. 1971. *J. Biol. Chem.* **246**:3817.

COHEN, S. S. 1970. *Am. Sci.* **58**:281.

COTTRELL, S. F., and C. J. AVERS. 1971. *In* Autonomy and Biogenesis of Mitochondria and Chloroplasts. N. K. Boardman et al., editors. North-Holland Publishing Company, Amsterdam. 481.

FORD, D. K., and G. YERGANIAN. 1958. *J. Natl. Cancer Inst.* **21**:393.

HAWLEY, E. S., and R. P. WAGNER. 1967. *J. Cell Biol.* **35**:489.

KOCK, J., and E. L. R. STOKSTAD. 1967. *Eur. J. Biochem.* **3**:1.

LINNANE, A. W., D. BIGGS, M. HUANG, and G. CLARK-WALKER. 1968. *In* Some Aspects of Yeast Metabolism. R. K. Mills, editor. Blackwell Scientific Publications Ltd., Oxford. 217.

OSUMI, M., and N. SANDO. 1969. *J. Electron Microsc.* **18**:47.

PICA-MATTOCCIA, L., and G. ATTARDI. 1972. *J. Mol. Biol.* **65**:465.

RABINOWITZ, M., and H. SWIFT. 1970. *Physiol. Rev.* **50**:376.
ROODYN, D. B., and D. WILKIE. 1968. Biogenesis of Mitochondria. Methuen and Co. Ltd., London.
ROSS, D. W., and W. K. SINCLAIR. 1972. *Cell Tissue Kinet.* **5**:1.
ROSS, D. W. 1972. Cellular and Mitochondrial Dynamics in Chinese Hamster Cells. Ph. D. Thesis, University of California, Berkeley. LBL-946.
SINCLAIR, W. K., and R. A. MORTON. 1963. *Nature* (*Lond.*). **199**:1158.
SINCLAIR, W. K., and D. W. ROSS. 1969. *Biophys. J.* **9**:1056.
TAUCHI, H., and T. SATO. 1966. *J. Gerontol.* **23**:454.